Liquid mean residence time (MRT) in rotating packed bed (RPB) by empirical correlation and residence time distribution (RTD) method using computational fluid dynamics (CFD) simulation

Abdul Zahir[a], Perumal Kumar*[a], Agus Saptoro[a], Angnes Ngieng Tze Tiong[a], Samreen Hameed[b], Milinkumar Shah[c]

[a] Department of Chemical and Energy Engineering, Curtin University Malaysia

[b]Department of Chemical, Polymer & Composite Material Engineering, University of Engineering and Technology, New Campus, Lahore

[c]Western Australia School of Mines: Mineral, Energy and Chemical Engineering, Curtin University, Bentley, Western Australia 6102, Australia

*p.kumar@curtin.edu.my

Abstract. Rotating packed bed (RPB) belongs to a HIGee technology, a process intensification device that can provide better mass transfer rate due to the generation of hyper-gravity under the influence of centrifugal force. While determining the efficiency of the RPB, the MRT of the liquid plays a vital role. The MRT of the RPB is very small and can be tuned in accordance with the mass transfer rate of the solvent to achieve the required outlet concentration of the absorbed gas. There exist two methods, i.e., empirical correlation and the residence time distribution (RTD) method. The applicability of both methods still needs to be investigated for better prediction of MRT in RPB. The current study compares the MRT of the two of the most widely employed techniques, i.e., MRT by empirical correlation and the RTD approach using the Computational Fluid Dynamics (CFD). The difference between the MRT by both methods lies between 30-38%. The results show that the RTD better predicts the MRT in the RPB as compared to the Burns empirical correlation.

1. Introduction

Rotating packed bed (RPB) is an advanced process intensification device that has paved its way into various chemical industries such as distillation [1], nanoparticle synthesis [2] and gas purification [3][4]. The centrifugal force, which tends to cause the rotational motion in the RPB, enhances the mass transfer efficiency up to 1-2 orders of magnitude due to intensified mixing at the gas-liquid interface as compared to the packed bed reactor [5]. The energy demand has increased dramatically in the last two decades due to industrialization advancements [6]. To fulfil those energy requirements, fossil fuel incineration is being used to serve this purpose [7]. However, the emission of CO_2 as a result of this incineration affects the global carbon cycle and is, therefore, considered one of the major causes of global warming [8]. Various remedial actions have been proposed to cope with this concern by adopting different techniques

such as adsorption [9], membrane separation [10], absorption [11] and cryogenics [12]. Among all the proposed techniques, absorption is one of the most reliable, economical, effective and mature carbon-capturing techniques [13].

In order to utilize the potential of RPB for CO_2 absorption, the mean residence time (MRT) in the RPB is crucial. The MRT of the solvent in the RPB is very small and therefore, it must be synchronized with the mass transfer rate in the RPB [14]. Thus, an accurate prediction of the MRT is one of the critical factors while designing the RPB and optimizing the operational parameters for CO_2 absorption. The MRT of the solvent can be calculated by using experimental methods using sensors or engineering devices. However, the experimental approach is expensive and the placement of sensors and the engineering devices in the RPB is challenging due to the complex packing structure of the RPB [15]. Computational Fluid Dynamics (CFD) is an advanced computational tool to study the hydrodynamics of the RPB. To accurately predict the hydrodynamics of the RPB, selecting the appropriate turbulence model is essential. Among various turbulence models, the SST k-omega turbulence model is the most effective model as compared to the other two-equation turbulence models [16]. To the best of our knowledge, no data exists in the scientific literature that compares the MRT by empirical correlation and RTD method using the CFD technique.

The current investigation aims to compare the MRT of the solvents, i.e., MEA and KPZ in the RPB by employing the Burns empirical correlation and the RTD method using the CFD. The flow of the liquid in the RPB was solved by employing the Reference Frame Model (RFM). The MRT was determined by for two different solvents, i.e., Monoethanolamine (MEA) and Piperazine (7.5% by weight of K_2CO_3) promoted potassium carbonate (KPZ) having different solution properties such as dynamic viscosity, density and surface tension.

2. CFD Model

2.1. Geometric model

The MRT study was performed using the RPB used in Yang et al. [17] experiments. Due to the unavailability of the packing details, i.e., packing type and structure, the generation of the exact same packing was practically not possible. The 2D geometric model was built by considering only the coaxial wires in the packing. The dimensional parameters of the 2D geometry are tabulated in Table 1.

Table 1: Dimensions of 2D CFD geometry

Inner diameter of the packing	42mm
Outer diameter of the packing	82mm
Inner diameter of RPB	38mm
Outer diameter of RPB	84 mm
Dimeter of the coaxial wire	0.5mm
Layers of packing wires	21
Circumferential distance of two adjacent wires	3.5mm
Radial distance of two adjacent wires	3.5mm
Surface area of the packing	478 1/m

2.2. Boundary conditions

The relative movement of the inlet with respect to the packing was controlled using the in-house developed User Defined Function (UDF) and the width of the inlet nozzle was set to 1mm. There were total of 10 pressure outlets and the width of each pressure outlet was 3mm. Each simulation was performed with no-slip boundary condition for the packing walls. The RPB was

initialized and patched with the solvent's volume fraction of 0 to ensure that there was only CO_2 in the RPB before the solvent was injected. The details of the boundary conditions are presented in Table 2.

Table 2: Boundary conditions for the MRT study

Variable	**MEA**	**KPZ**
Solvent Concentration	30 and 60 wt.%	15 and 27.5 wt.%
Rotational Speed	1000 and 1500 rpm	1000 and 1500 rpm
Solvent inlet velocity	1.22 and 2.045 m/s	1.22 and 2.045 m/s
Contact angle	0 and 75°	0 and 75°

2.3. Solution procedure

All the simulation studies were performed as the transient simulation using Ansys Fluent (2020R1). The pressure-velocity coupling was solved by the PISO algorithm. The volume fraction was computed by the Geo-Reconstruct discritization method. The CFD simulations were run for 5×10^4 time steps with a time step size of 1×10^{-5}. A maximum of 30 iterations per time step were performed to ensure the solution convergence.

2.4. Computational Grid

Computational grid number is very important and can affect the simulated results' accuracy. The effect of the boundary layers on the liquid flow was encountered by creating a dense mesh around the packing surface. Using the Ansys meshing software, different mesh numbers ranging from 0.12-0.94M were generated in the computational domain. The liquid holdup at different mesh sizes was calculated and compared, as shown in Figure 1. As the Figure 1 portrays that, the liquid holdup increases up to 28% when the mesh number increased from 0.12M to 0.42M. However, no significant change in the liquid holdup can be observed when the cell count for computational grid was further increased from 0.42M cells which reveals that 0.42M cells are fine enough to predict the liquid holdup in the RPB.

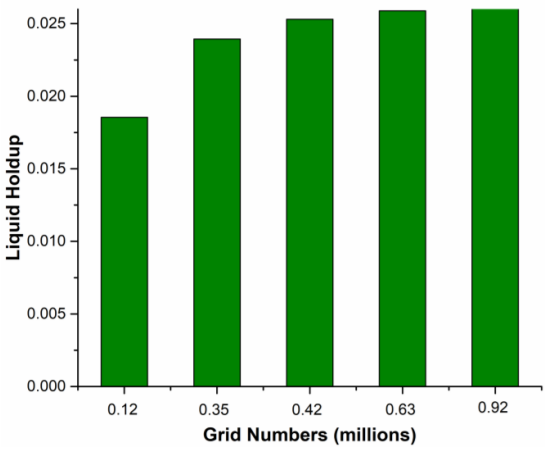

Figure 1: Effect of grid numbers on the liquid holdup

2.5. Model validation

The model validation of the 2D CFD model was done using water as the secondary phase and air as the primary phase. The liquid holdup at three different rotational speeds, i.e., 500, 1000 and 1500 RPMs at 1.53 m/s solvent inlet velocity and 30° liquid-packing contact angle were calculated. The simulated results were compared with the experimental data of Yang et al. [17] and the empirical correlation proposed by Burns et al. [18], which can be expressed as follow.

$$\boldsymbol{\varepsilon_L} = 0.039\left(\frac{g}{g_o}\right)^{-1/2}\left(\frac{U}{U_o}\right)^{0.6}\left(\frac{v}{v_o}\right)^{0.22} \quad (1)$$

Where g (m.s^{-2}) is the centrifugal acceleration, g_o (m.s^{-2}) is the characteristic centrifugal acceleration, U (m.s^{-1}) is the superficial velocity, U_o (m.s^{-1}) is the characteristic superficial velocity, v (m^2.s^{-1}) is the kinematic viscosity of the liquid and v_o (m^2.s^{-1}) is the kinematic viscosity of the liquid.

2.6. Liquid Mean Residence Time (MRT)

2.6.1. Empirical correlation. The MRT was calculated using the equation proposed by Burns et al. [18]

$$\boldsymbol{\varepsilon_L} = \frac{A_{liq}}{A_{total}} \quad (2)$$

$$\mathbf{t} \cong \frac{\boldsymbol{\varepsilon_L}}{\left(\frac{\mathbf{u_o d}}{\boldsymbol{\pi}(\mathbf{r_o}+\mathbf{r_1})}\right)}(\mathbf{r_o}-\mathbf{r_1}) \quad (3)$$

Where, $\boldsymbol{\varepsilon_L}$ is the liquid holdup, $\boldsymbol{A_{liq}}$ and $\boldsymbol{A_{total}}$ are the area of the liquid in the RPB and the total area of the RPB, respectively, $\boldsymbol{u_o}$is the inlet velocity of solvent, i.e., MEA and KPZ, $\boldsymbol{d}$ (mm) is the width of the injection nozzle, $\boldsymbol{r_o}$and $\boldsymbol{r_1}$are the inner and outer radius of the packing, respectively.

2.6.2. Residence Time Distribution (RTD). Once the pseudo-steady state was achieved, the tracer having the same solution properties as of the solvent was injected into the RPB for a very short interval of time, i.e., 0.001s by changing the volume fraction of the tracer at the inlet to unity. After 0.001s, the volume fraction of the tracer was reset to 0 and the solvent was reinjected immediately and the concentration of the tracer at the outlet was monitored until the complete tracer came out of the RPB. The MRT was calculated using the following formula [19]

$$\bar{\boldsymbol{t}} = \frac{\sum \boldsymbol{F_i t_i}}{\sum \boldsymbol{F_i}} \quad (3)$$

Where, $\boldsymbol{F_i}$ is the dimensionless concentration of the solvent, i.e., MEA and KPZ and $\boldsymbol{t_i}$ is the flow time.

3. Results and Discussion

3.1. Model Validation

As can be seen in Figure 2, the simulated results show a better prediction of the liquid holdup as compared to the Burn empirical correlation. This is because the Burns empirical correlation was developed using the conductivity measurements and therefore, the droplets which reside freely within the vicinity of the packing were ignored during the correlation development. Moreover, the error in the CFD simulated results is because the liquid droplets entrapped at the junction point of coaxial and concentric wires are not considered in the 2D model of the geometry.

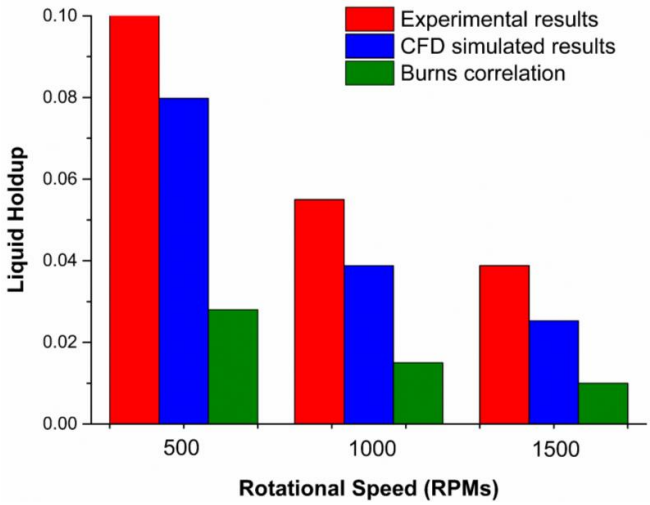

Figure 2: Comparison of simulated results with the experimental data of Yang. et al. [17] *and Burns correlation*

3.2. Liquid Mean Residence Time (MRT)

The RTD plot of both MEA and KPZ are shown in Figure 3 and the results of MRT by the empirical correlation and RTD are presented in Figure 3: Residence Time Distribution (RTD) plot of MEA and KPZ

Table 3. As can be seen in Figure 3: Residence Time Distribution (RTD) plot of MEA and KPZ Table 3 the MRT of MEA is less than the KPZ. This low MRT value of MEA is due to the relatively low frictional forces between MEA molecules which increases the deformation rate compared to the KPZ when the RPB packing exerts the shear force. It can also be observed that with the decrease in the solvent concentration, the MRT of both MEA and KPZ decreases. This reduction in the MRT is also associated with the low viscosity values as compared to the high concentrations. While at low γ° the surface of the packing become hydrophilic and the wettability of the packing decreases which also reduces the adhesion of solvents with the packing and thus shows a low MRT.

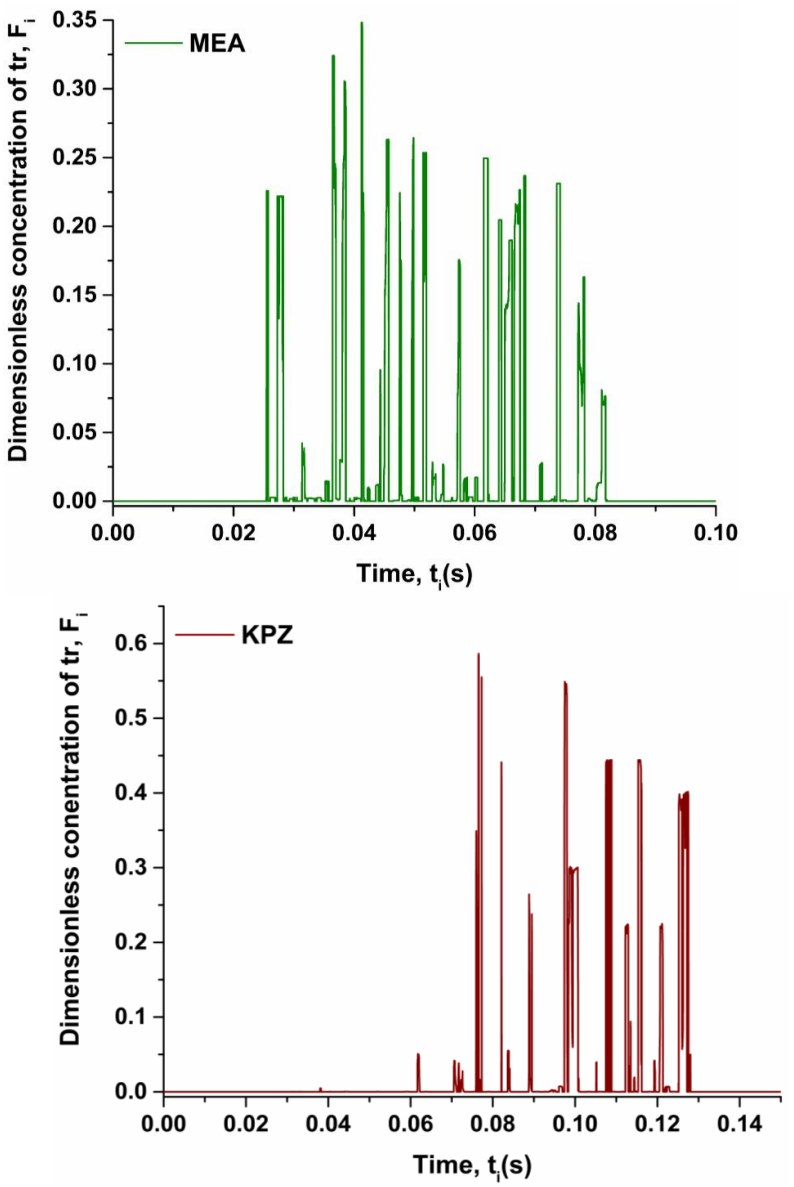

Figure 3: Residence Time Distribution (RTD) plot of MEA and KPZ

Table 3: MRT by empirical correlation and RTD

Sr. No	N (RPMs)	u_o (m/s)	S.C (%)	γ° (degree)	MTR_{EC}	MTR_{RTD}	ΔMRT
MEA							
1	1000	2.045	60	75	0.092	0.139	0.047
2	1500	1.22	30	0	0.056	0.080	0.024
KPZ							

1	1000	2.045	27.5	75	0.259	0.260	0.001
2	1500	1.22	15	0	0.072	0.110	0.038

N= Rotational speed, u_o= Inlet velocity, S.C= Solvent Concentration, γ° = Contact angle

It can be observed from Figure 3: Residence Time Distribution (RTD) plot of MEA and KPZ
Table 3 that the low MRT values by the empirical correlation are due to the employment of the 2D geometry of RPB for the CFD simulations which do not consider the concentric wires in the packing structure and therefore, the liquid entrapped between the intersection of axial and concentric wires cannot be predicted using the 2D geometry. Another reason which might be the cause of this difference is the assumptions that Burns et al. [18] made during the correlation development.

4. Conclusion

The comparison of liquid MRT by empirical correlation and the Residence Time Distribution (RTD) method has been performed using the Computational Fluid Dynamics (CFD) simulation. Both MTR_{EC} and MTR_{RTD} follow the same trend under the same operational conditions. However, the Burns correlation for the MTR_{EC} is based on assumptions that limit its prediction accuracy for the MRT. The results reveal that the MTR_{RTD} by RTD method using CFD simulation can predict the MRT of the RPB more accurately than the empirical correlation. However, the RTD method requires more computational time as compared to the Burns correlation. The outcomes of this research can be applied to the industrial RPB using the 3D CFD model for tuning mean residence time (MRT) in accordance with the mass transfer rate of the solvent.

References

[1] R. J. Prada, E. L. Martínez, and M. R. W. Maciel, "Computational Study of a Rotating Packed Bed Distillation Column," *Comput. Aided Chem. Eng.*, vol. 30, pp. 1113–1117, Jan. 2012, doi: 10.1016/B978-0-444-59520-1.50081-6.

[2] Q. Liu, Y. Pu, Z. Zhao, J. Wang, and D. Wang, "Synthesis of Silver Sulfide Quantum Dots Via the Liquid–Liquid Interface Reaction in a Rotating Packed Bed Reactor," *Trans. Tianjin Univ.*, vol. 26, no. 4, pp. 273–282, Aug. 2020, doi: 10.1007/S12209-019-00228-5.

[3] J. Guo, W. Jiao, G. Qi, Z. Yuan, and Y. Liu, "Applications of high-gravity technologies in gas purifications: A review," *Chinese J. Chem. Eng.*, vol. 27, no. 6, pp. 1361–1373, Jun. 2019, doi: 10.1016/J.CJCHE.2019.01.011.

[4] F. Ghadyanlou, A. Azari, and A. Vatani, "A Review of Modeling Rotating Packed Beds and Improving Their Parameters: Gas–Liquid Contact," *Sustain. 2021, Vol. 13, Page 8046*, vol. 13, no. 14, p. 8046, Jul. 2021, doi: 10.3390/SU13148046.

[5] K. N. Finney, M. Akram, M. E. Diego, X. Yang, and M. Pourkashanian, "Carbon capture technologies," *Bioenergy with Carbon Capture Storage Using Nat. Resour. Sustain. Dev.*, pp. 15–45, Jan. 2019, doi: 10.1016/B978-0-12-816229-3.00002-8.

[6] P. Pakzad, M. Mofarahi, M. Ansarpour, M. Afkhamipour, and C.-H. Lee, "CO2 absorption by common solvents," *Adv. Carbon Capture*, pp. 51–87, Jan. 2020, doi: 10.1016/B978-0-12-819657-1.00003-7.

[7] S. Paraschiv and L. S. Paraschiv, "Trends of carbon dioxide (CO2) emissions from fossil fuels combustion (coal, gas and oil) in the EU member states from 1960 to 2018," *Energy Reports*, vol. 6, pp. 237–242, Dec. 2020, doi: 10.1016/J.EGYR.2020.11.116.

[8] W. M. Budzianowski, "Modelling of CO2 content in the atmosphere until 2300: Influence of energy intensity of gross domestic product and carbon intensity of energy," *Int. J. Glob. Warm.*, vol. 5, no. 1, pp. 1–17, 2013, doi: 10.1504/IJGW.2013.051468.

[9] L. Giraldo, D. P. Vargas, and J. C. Moreno-Piraján, "Study of CO2 Adsorption on Chemically Modified Activated Carbon With Nitric Acid and Ammonium Aqueous," *Front. Chem.*, vol. 8, p. 1007, Nov. 2020, doi: 10.3389/FCHEM.2020.543452/BIBTEX.

[10] C. Castel, R. Bounaceur, and E. Favre, "Membrane Processes for Direct Carbon Dioxide Capture From Air: Possibilities and Limitations," *Front. Chem. Eng.*, vol. 0, p. 17, Apr. 2021, doi: 10.3389/FCENG.2021.668867.

[11] B. Lv, B. Guo, Z. Zhou, and G. Jing, "Mechanisms of CO2 Capture into Monoethanolamine Solution with Different CO2 Loading during the Absorption/Desorption Processes," *Environ. Sci. Technol.*, vol. 49, no. 17, pp. 10728–10735, Sep. 2015, doi: 10.1021/ACS.EST.5B02356/ASSET/IMAGES/MEDIUM/ES-2015-02356N_0010.GIF.

[12] C. Font-Palma, D. Cann, C. Udemu, and O. García, "Review of Cryogenic Carbon Capture Innovations and Their Potential Applications," *C 2021, Vol. 7, Page 58*, vol. 7, no. 3, p. 58, Jul. 2021, doi: 10.3390/C7030058.

[13] C. Zhang, "Absorption principle and techno-economic analysis of CO2 absorption technologies: A review," *IOP Conf. Ser. Earth Environ. Sci.*, vol. 657, no. 1, Feb. 2021, doi: 10.1088/1755-1315/657/1/012045.

[14] K. Guo, F. Guo, Y. Feng, J. Chen, C. Zheng, and N. C. Gardner, "Synchronous visual and RTD study on liquid flow in rotating packed-bed contactor," *Chem. Eng. Sci.*, vol. 55, no. 9, pp. 1699–1706, May 2000, doi: 10.1016/S0009-2509(99)00369-3.

[15] W. Zhang, P. Xie, Y. Li, L. Teng, and J. Zhu, "Hydrodynamic characteristics and mass transfer performance of rotating packed bed for CO2 removal by chemical absorption: A review," *J. Nat. Gas Sci. Eng.*, vol. 79, no. May, p. 103373, 2020, doi: 10.1016/j.jngse.2020.103373.

[16] P. Xie, X. Lu, X. Yang, D. Ingham, L. Ma, and M. Pourkashanian, "Characteristics of liquid flow in a rotating packed bed for CO2 capture: A CFD analysis," *Chem. Eng. Sci.*, vol. 172, pp. 216–229, Nov. 2017, doi: 10.1016/j.ces.2017.06.040.

[17] Y. Yang *et al.*, "A noninvasive X-ray technique for determination of liquid holdup in a rotating

packed bed," *Chem. Eng. Sci.*, vol. 138, pp. 244–255, Dec. 2015, doi: 10.1016/J.CES.2015.07.044.

[18] J. R. Burns, J. N. Jamil, and C. Ramshaw, "Process intensification: operating characteristics of rotating packed beds — determination of liquid holdup for a high-voidage structured packing," *Chem. Eng. Sci.*, vol. 55, no. 13, pp. 2401–2415, Jul. 2000, doi: 10.1016/S0009-2509(99)00520-5.

[19] T. Y. Guo, K. P. Cheng, L. X. Wen, R. Andersson, and J. F. Chen, "Three-Dimensional Simulation on Liquid Flow in a Rotating Packed Bed Reactor," *Ind. Eng. Chem. Res.*, vol. 56, no. 28, pp. 8169–8179, Jul. 2017, doi: 10.1021/ACS.IECR.7B01759.